Finite-Orbit-Width Effects on Energetic-Particle-Induced Geodesic Acoustic Mode[*)]

Kazuhiro MIKI and Yasuhiro IDOMURA

Japan Atomic Energy Agency, 178-4-4 Wakashiba, Kashiwa, Chiba 277-0871, Japan

We identify linear properties of the energetic-particle-induced geodesic acoustic mode (EGAM) using eigenmode analysis based on the gyrokinetic theory. From the perturbed gyrokinetic equation with energetic particles, we derive a dispersion relation of the EGAM. The behaviors of the roots vary depending on the safety factor. Taking into account of the finite-orbit-width (FOW) effects, we examine variations of the growth rates of the EGAM for various beam intensities. The analyses indicate that the FOW effects are small, within several percent of the growth rates, for experimentally relevant radial wave numbers.

1. Introduction

Understanding of energetic particles physics is of great interest in the burning plasmas. The fusion reaction produces 3.5 MeV alpha particles, while neutral beam injection (NBI) induce the energetic particles as well. Such energetic particles induce various mode excitations [1, 2].

Recent studies have disclosed the existence of energetic-particles-induced modes with $n = 0$, where n is a toroidal mode number. DIII-D experiments have found mode excitation in the presence of the counter NBI [3]. The mode structure is identical to that of geodesic acoustic mode (GAM) [4], but its frequency is about a half of that of the GAM. Analyses based on a hybrid model including MHD modes and energetic particles [5] have revealed a new GAM-like mode, which has a disparate branch from the GAM. The mode is referred to as energetic-particle-induced geodesic acoustic mode (EGAM).

The EGAM has so far been studied with the hybrid, drift kinetic and gyrokinetic models [3, 5–12]. Notice that the hybrid model treatments have not considered kinetic effects of the bulk particles themselves. Thus, they neglect the Landau damping effects on the EGAM resonances. If one considers a damping of the EGAM due to higher order resonances, naturally one will come across finite-orbit-width (FOW) effects. The FOW effects are essential for estimating the damping rate of GAM [13]. To see its impact on the EGAM, we extend the gyrokinetic theory of EGAM by taking account of the FOW effects.

In this paper, we identify linear properties of the EGAM, in terms of eigenmode analyses, for a given bump-on-tail particle distribution. A perturbed gyrokinetic equation together with a quasi-neutrality condition closes the system to derive a dispersion relation of the EGAM. We assess the FOW effects on the resonance of EGAM.

The reminder of this paper is the followings. In Sec. 2, we derive the dispersion relation of the EGAM based on the linear perturbed gyrokinetic equation with energetic particles. In Sec. 3, we discuss parametric characteristics of the roots of GAM and EGAM. In Sec. 4, we conclude this work and remark the further validation on numerical simulations.

2. Derivation of the Eigenmodes of EGAM Based on the Gyrokinetic Theory

We use the toroidal coordinates (r, θ, ζ), assuming tokamak plasmas. For a given equilibrium distribution $F_0(\mathbf{R}, \mu, v_\parallel)$, the linear perturbed gyrokinetic equation for the zonal component with the perpendicular wave number $k_\perp = k_r \nabla r$ is given by [14]

$$(\partial_t + v_\parallel b \cdot \nabla + i\omega_D) g_{k_\perp} = -\frac{e}{m v_\parallel} \frac{\partial F_0}{\partial v_\parallel} J_0 \frac{\partial \phi_{k_\perp}}{\partial t}, \quad (1)$$

where J_0 is the zeroth-order Bessel function. $\omega_D = v_\parallel \mathbf{b} \cdot \nabla(k_r d_r)$ is the magnetic drift frequency, where $d_r = (q/\omega_{ci})(v_\parallel + v_\perp^2/2v_\parallel)\cos\theta$ and $\omega_{ci} = qB/m$. $\mu \equiv m v_\perp^2/(2B)$ is the magnetic moment. We assume radial homogeneity, so that a term proportional to $\partial_r F_0$ is dropped in Eq. (1). We also neglect a term of the mirror force. The equilibrium distribution function F_0 satisfies a local Maxwellian.

In reference to Ref. [9], we adopt a bump-on-tail distribution for F_0, written as

$$F_0 = \left(\frac{1}{1 + n_h}\right) F_{0,\text{bulk}} + \left(\frac{n_h}{1 + n_h}\right) F_{0,\text{beam}}, \quad (2a)$$

author's e-mail: miki.kazuhiro@jaea.go.jp

$$F_{0,\text{bulk}} = \frac{1}{(2\pi v_{\text{ti}}^2)^{3/2}} \exp\left(-\frac{m_i v_\parallel^2 + 2\mu B}{T_i}\right), \qquad (2b)$$

$$
\begin{aligned}
F_{0,\text{beam}} = &\frac{1}{2} \frac{1}{(2\pi \hat{T}_h v_{\text{ti}}^2)^{3/2}} \\
&\times \left[\exp\left(-\frac{m_i(v_\parallel - v_0)^2 + 2\mu B}{2 T_i \hat{T}_h}\right)\right. \\
&\left.+ \exp\left(-\frac{m_i(v_\parallel + v_0)^2 + 2\mu B}{2 T_i \hat{T}_h}\right)\right]. \quad (2c)
\end{aligned}
$$

We represent T_i to be the temperature of *the bulk particles*. Also we define $v_{\text{ti}}^2 = T_i/m_i$. Other important parameters are a beam intensity n_h, which is defined as the proportion of the number of the energetic particles to that of the bulk ones, a beam velocity v_0, which we here choose $v_0 = 4v_{\text{ti}}$, and a normalized beam temperature, $\hat{T}_h$, which is chosen as unity for simplicity.

The r.h.s. of Eq. (1) can be rewritten as

$$-\frac{e}{mv_\parallel}\frac{\partial F_0}{\partial v_\parallel} J_0 \frac{\partial \phi_{k_\perp}}{\partial t} = Y J_0 F_0 \frac{e}{T_i}\frac{\partial \phi_{k_\perp}}{\partial t}, \qquad (3)$$

where $Y \equiv (T_i/mv_\parallel)F^{-1}(\partial_{v_\parallel} F_0)$. Here, Y measures a deviation from the Maxwellian distributions (e.g. for $n_h = 0$, $Y/(T_i/m_i v_\parallel) = 1$). The destabilization of the EGAM occurs in the region $Y < 0$. The EGAM grows when a parallel velocity gradient of the distribution function is negative at the resonance.

The quasineutrality condition is given by

$$
\begin{aligned}
&\int \mathrm{d}^3 v J_0 \delta f_{i,k_\perp}^{(g)} + \int \mathrm{d}^3 v Y F_{i0}(1 - J_0^2)\frac{e\phi_{k_\perp}}{m_i} \\
&= \int \mathrm{d}^3 v \delta f_{e,k_\perp}, \qquad (4)
\end{aligned}
$$

where $\delta f_{i,k_\perp}^{(g)}$ is the perturbed gyrocenter distribution function for ion species, $F_{i0} = F_0$ is the equilibrium distribution function for ion species, and $\delta f_{e,k_\perp}$ is the electron perturbed distribution function. The electrons are assumed to be adiabatic. Representing T_e as the electron temperature, we yield (r.h.s of Eq. (4)) $= \delta n_e = n_0 e\phi_{k_\perp}/T_e$ for $(m,n) \neq (0,0)$, or $\delta n_e = 0$ for $(m,n) = (0,0)$, where $T_i = T_e$.

Taking into account of modes with $n = 0, m = 0, \pm 1$, a symmetry in the poloidal modes, and $\omega_D \ll \omega_t$, Eqs. (1 - 4) yield a linear dispersion relation for EGAMs,

$$
\begin{aligned}
D(\hat{\omega}) = &-i\hat{\omega} - i\frac{q^2}{4}\left\{(4\hat{\omega})Z_1^{-1}Z_{2,0}^2 - Z_{4,0}\right. \\
&-i\left(\frac{k_r \rho_i q}{\sqrt{2}}\right)^2 \mathrm{Im}\left[Z_{4,\text{FOW}} + Z_1^{-1}\left(Z_{3,0}Z_{2,\text{FOW}} + Z_{2,0}Z_{3,\text{FOW}}\right)\right] \\
&\left.+ O\left[\left(\frac{k_r \rho_i q}{\sqrt{2}}\right)^4\right]\right\} = 0. \qquad (5)
\end{aligned}
$$

Here, q is the safety factor, ρ_i is the ion Larmor radius, and Z_1, $Z_{2,0}$, $Z_{4,0}$, $Z_{2,\text{FOW}}$, $Z_{3,\text{FOW}}$, $Z_{4,\text{FOW}}$ are the coefficients related to resonance integrals. They are calculated from

the following resonance integrals:

$$Z_1 = -\frac{T_i}{T_e} + \frac{1}{\sqrt{\pi}}\int \mathrm{d}\hat{\zeta} Y(\hat{\zeta}) F_{i0}\left[\frac{\hat{\zeta}}{\hat{\omega} - \hat{\zeta}}\right], \qquad (6a)$$

$$Z_{2,0} = \frac{1}{\sqrt{\pi}}\int \mathrm{d}\hat{\zeta} Y F_{i0}\frac{1}{2}\left[\frac{1 + 2\hat{\zeta}^2}{\hat{\omega} - \hat{\zeta}}\right], \qquad (6b)$$

$$
\begin{aligned}
Z_{4,0} = &\frac{1}{\sqrt{\pi}}\int \mathrm{d}\hat{\zeta} Y(\hat{\zeta}) F_{i0} \\
&\cdot\left(\frac{\hat{\zeta}}{\hat{\omega} + \hat{\zeta}} + \frac{\hat{\zeta}}{\hat{\omega} - \hat{\zeta}}\right)\left(\frac{1}{\hat{\zeta}} + 2\hat{\zeta} + 2\hat{\zeta}^3\right), \qquad (6c)
\end{aligned}
$$

$$
\begin{aligned}
Z_{2,\text{FOW}} = &\frac{1}{\sqrt{\pi}}\int \mathrm{d}\hat{\zeta} Y F_{i0} \\
&\cdot\frac{1}{2}\left[\frac{(3 + 6\hat{\zeta}^2 + 6\hat{\zeta}^4 + 4\hat{\zeta}^6)}{\hat{\zeta}^2(\hat{\omega} - 2\hat{\zeta})}\right], \qquad (6d)
\end{aligned}
$$

$$
\begin{aligned}
Z_{3,\text{FOW}} = &\frac{1}{\sqrt{\pi}}\int \mathrm{d}\hat{\zeta} Y F_{i0}\left[\frac{\hat{\zeta}}{\hat{\omega} + 2\hat{\zeta}} - \frac{\hat{\zeta}}{\hat{\omega} - 2\hat{\zeta}}\right] \\
&\cdot\left(\frac{3}{\hat{\zeta}^2} + 6 + 6\hat{\zeta}^2 + 4\hat{\zeta}^4\right), \qquad (6e)
\end{aligned}
$$

$$
\begin{aligned}
Z_{4,\text{FOW}} = &\frac{1}{\sqrt{\pi}}\int \mathrm{d}\hat{\zeta} Y F_{i0}\left[\frac{\hat{\zeta}}{\hat{\omega} + 2\hat{\zeta}} + \frac{\hat{\zeta}}{\hat{\omega} - 2\hat{\zeta}}\right] \\
&\cdot 2\left(\frac{3}{\hat{\zeta}^3} + frac{6}{\hat{\zeta}} + 6\hat{\zeta} + 4\hat{\zeta}^3 + 2\hat{\zeta}^5\right). \qquad (6f)
\end{aligned}
$$

Here, ω and ζ are normalized by v_{ti}/Rq and R is the major radius $Z_{2,\text{FOW}}$, $Z_{3,\text{FOW}}$, $Z_{4,\text{FOW}}$ are the contributions from the FOW effects proportional to $(qk_r\rho_i)^2$. By assuming $|\mathrm{Im}[\omega]| \ll |\mathrm{Re}[\omega]|$, we keep only the imaginary parts of $Z_{2,\text{FOW}}$, $Z_{3,\text{FOW}}$, $Z_{4,\text{FOW}}$. The FOW contribution in the real part is negligible in order of $(k_r\rho_i q)^2$, while that in the imaginary part may not be negligible, since the lower resonant frequency and accordingly the larger population of resonant ions are produced due the FOW effects [13]. Note that in the limit of $n_h = 0$, Eq. (5) is identical to the dispersion relation of the GAM in Ref. [13]. We also note that the obtained dispersion relation is identical to that obtained in Ref. [12], without the FOW effects.

In this analysis, we take only (0,0) and (1,0) modes, but ones with $|m| \geq 2$, in accordance with Ref. [13]. This approximation can be valid, since the mode frequency of the EGAM is the same order as that of the standard GAM. Furthermore, we compare the analytical results with those obtained from numerical simulations GT5D [15] (See Fig. 5). The analytical results are well consistent with the numerical ones.

3. Eigenmode Analyses of the EGAM with the FOW Effects

Numerically solving the dispersion relation of Eq. (5) for various n_h and q, we can find roots with the mode structure with $m = 1$ and $n = 0$. Without the beam injection we see a single root in higher frequency and damping region. We find that the root is consistent with the GAM. Including the beam injection, we identify a new mode emerging. We possibly identify the new root as the EGAM. Scanning on n_h, we see that the two distinct roots move on the
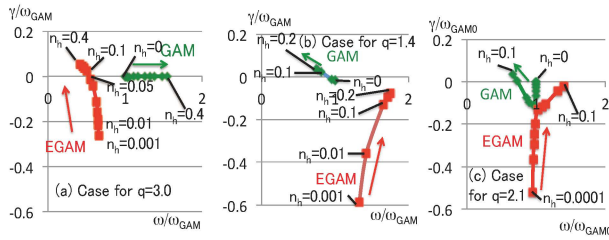
Fig. 1   Plots of the GAM (rectangular) and EGAM (diamond) roots mapping on the complex frequency plane (ω, γ), for various beam intensities, in (a) $q = 3.0$, (b) $q = 1.4$, and (c) $q = 2.1$ cases. Here, $k_r = 0$ (i.e. no FOW effects) is chosen.

Fig. 2   For a fixed beam intensity $n_h = 0.15$ and the FOW effects ($k_r \rho_i = 0.02$), plots of growing and damping roots for various q ($q = 1.3 \text{-} 3.0$). Labels of EGAM/GAM are switched at $q = 2.1$. Either EGAM or GAM, one mode is growing and the other is damping. We also plot the evolution of the damping mode without FOW.

Fig. 3   Plots of the growth and damping rates of the analytical roots as a function of q, for cases with and without the FOW effects.

complex frequency plane continuously. Thus, we can label each mode either GAM or EGAM, by plotting the evolution of the roots from the zero-limit of the beam intensity.

Figure 1 illustrates evolutions of the calculated roots mapping on the complex frequency plane (ω, γ), where ω is a real frequency and γ is a growth rate normalized by the standard GAM frequency ω_{GAM}. For simplicity, we here do not consider the FOW effects, but these findings are consistent for cases including the FOW effects. In the higher q case, as n_h increases, an EGAM root becomes a growing mode, while a GAM root keeps a damping one (See Fig. 1 (a)). The real frequencies of the EGAM decreases with increasing n_h, while those of the GAM increases. We also see the frequency of the EGAM is mostly half of that of the standard GAM, consistent with the previous literature [5, 7].

The behaviors of the two roots are qualitatively changed depending on q. As seen in Fig. 1 (b), as n_h increases, the GAM root becomes a growing mode for the lower q case, while the EGAM keeps damping one. So we find that bifurcation of the growing mode is expected depending on q.

Then, what happened in the critical q? We plot the evolutions of the roots in the case for the intermediate q ($q = 2.1$) in Fig. 1 (c). For $n_h = 0.003 \text{-} 0.004$, the two roots are very close. This observation indicates that the two branches cross each other by a reconnection of the two roots. Thus, decreasing q below the critical value or $q \sim 2.1$, the EGAM roots become damping modes and the GAM ones become growing modes. A similar bifurcation is also analyzed in Ref. [5].

We investigate the root evolution for various q ($q = 1.3 \text{-} 3.0$) and the fixed beam intensity $n_h = 0.15$ in Fig. 2. Notably, either the growing or damping modes are aligned continuously, though their origins are different depending on q. The growing mode maximizes its growth rate at $q \sim 1.8 \text{-} 2.0$. The damping mode minimizes its damping rates at $q \sim 2.3$. Increasing q, the real frequencies of both the growing and damping mode decreases.

We here use $k_r \rho_i = 0.02$ on plotting the damping mode including the FOW effects in Fig. 2. We find a signifi-

cant difference of the damping modes with and without the FOW effects for the higher q ($q > 2.3$).
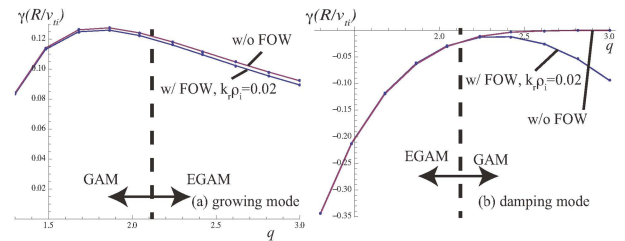
Continuously tracing roots as a function of q, we plot the behaviors of both growing and damping roots, in Fig. 3. For the growing mode, the difference, due to the FOW, is small, within several %. On the other hand, the difference of the damping rate is significant, especially for the case for the GAM, i.e. $q > 2.1$. Thus, we conclude that the effects of the FOW on the EGAM are weak for the experimentally relevant parameter.

In Fig. 4, we plot the growth rates of the EGAM for cases of $q = 3.0$ with various beam intensities, $n_h = 0.03 \text{-} 0.2$. We compare cases with and without the FOW effects. The results indicate that there is almost no difference for the experimentally relevant parameters. The difference is, at most, several percent.

In Fig. 5, we examine how much the FOW affects the EGAM and GAM in the case with $q = 3.0$ and $n_h = 0.15$. For the assessment of the FOW effects, we use typically $k_r \rho_i \sim 0.02 \text{-} 0.06$. For the EGAM, reduction of the growth rate is of order $(k_r \rho_i q)^2$. We compare the growth rates of the EGAM obtained from the eigenmode analyses with those from the GT5D simulations, showing consistency.

On the other hand, scan of the GAM damping rate exhibits significance of the FOW effects. Since the higher-q
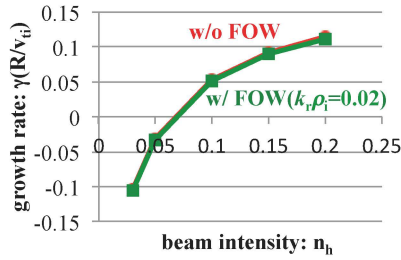
Fig. 4 Plots of the growth rate of the EGAM as a function of beam intensity n_h, fixed $q = 3.0$, for cases with and without the FOW effects. The difference is quite small, within several %.
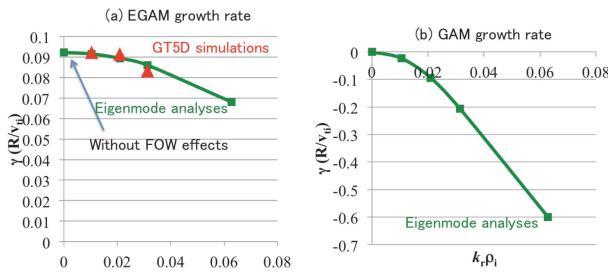
Fig. 5 Plots of (a) growth rates and (b) damping rates of the EGAM and GAM, respectively, as a function of $k_r\rho_i$, fixed $q = 3.0$ and $n_h = 0.15$. We compare the results obtained from the eigenmode analysis with those obtained from the initial value problem calculated by GT5D.

damping rate without the FOW effects are almost negligible due to the proportionality of the damping rate to $\exp(-q^2\omega^2 R^2/2v_{ti}^2)$. Whereas, the FOW involves an additional damping term proportional to $(qk_r\rho_i)^2\exp[-q^2\omega^2 R^2/(8v_{ti}^2)]$, due to the resonance $1/(\hat{\omega} - 2\zeta)$ of Eqs. (6d) - (6f).

4. Conclusions

We have investigated the linear properties of the EGAM. Together with the quasi-neutrality, we have solved $m = 0, \pm1$, $n = 0$ modes of the linear perturbed gyrokinetic equations. We have derived the dispersion relation of the EGAM and GAM including the energetic particles. Here,

bump-on-tail distributions represent the energetic particles. We have taken into account of the finite-orbit-width (FOW) effects on the EGAM. Obtained results are the followings: i) Including the energetic particles, a new root emerges, besides the original GAM root. The new root is the EGAM, driven by the beam injection. ii) Depending on q, evolutions of the two distinct roots can vary. For higher q, the EGAM becomes a growing mode. On the other hand, for lower q, the GAM becomes a growing one. For the intermediate or critical q, typically at $q \sim 2.1$, the two roots reconnect with each other. iii) The FOW effects on the EGAM are relatively weak, within the several percent, for experimentally relevant parameters. For larger $k_r\rho_i$, the difference may be significant. The difference of the GAM damping rates with and without the FOW effects are significant, since without the FOW effects the Landau damping of the GAM is almost negligible at high q. The further general reason why significance of the FOW effects only on the GAM roots is put on future works.

[1] F. Zonca and L. Chen, Phys. Rev. Lett. **68**, 592 (1992).
[2] H.L. Berk *et al.*, Phys. Rev. Lett. **87**, 185002 (2001).
[3] R. Nazikian *et al.*, Phys. Rev. Lett. **101**, 185001 (2008).
[4] N. Winsor *et al.*, Phys. Fluids **11**, 2448 (1968).
[5] G.Y. Fu, Phys. Rev. Lett. **101**, 185002 (2008).
[6] H. Wang *et al.*, Phys. Rev. Lett. **110**, 155006 (2013).
[7] Z. Qiu *et al.*, Plasma Phys. Control. Fusion **52**, 095003 (2010).
[8] H.L. Berk and T. Zhou, Nucl. Fusion **50**, 035007 (2010).
[9] D. Zarzoso *et al.*, Phys. Plasmas **19**, 022102 (2012).
[10] D. Zarzoso *et al.*, Phys. Rev. Lett. **110**, 125002 (2013).
[11] D. Zarzoso *et al.*, Nucl. Fusion **54**, 103006 (2014).
[12] J.-B. Girado *et al.*, Phys. Plasmas **21**, 092507 (2014).
[13] H. Sugama and T.-H. Watanabe, Phys. Plasmas **13**, 012501 (2006).
[14] E.A. Frieman and L. Chen, Phys. Fluids **25**, 502 (1982).
[15] Y. Idomura *et al.*, Nucl. Fusion **49**, 065029 (2009).